Vibrational signatures for low-energy intermediate-sized Si clusters

Mark R. Pederson

Complex Systems Theory Branch, Naval Research Laboratory, Washington, D.C. 20375

Koblar Jackson

Department of Physics, Central Michigan University, Mt. Pleasant, Michigan 48859

D. V. Porezag, Z. Hajnal and Th. Frauenheim

Department of Physics, Chemnitz University of Technology, Chemnitz, Germany

(Received 26 February 1996)

We report low-energy *locally stable* structures for the clusters Si_{20} and Si_{21}. The structures were obtained by performing geometry optimizations within the local density approximation. Our calculated binding energies for these clusters are larger than any previously reported for this size regime. To aid in the experimental identification of the structures, we have computed the full vibrational spectra of the clusters, along with the Raman and IR activities of the various modes using a recently developed first-principles technique. These represent, to our knowledge, the first calculations of Raman and IR spectra for Si clusters of this size. [S0163-1829(96)06227-3]

Interest in the properties of Si clusters has grown in recent years, both as a result of the drive toward design and miniaturization in the electronics industry, and due to the many interesting and surprising properties of atomic clusters that have emerged from early experimental work.[1] A crucial problem in this area involves the structure of the intermediate-sized clusters. The lowest-energy structures for small Si clusters ($N \leq 13$) appear well established by calculations[2–4] and for $N \leq 10$, experimental Raman spectra have confirmed these geometries.[5] At the other end of the size spectrum, large clusters are expected to take on bulklike structures. Between these limits, the structures of the intermediate-sized clusters are not known. The basic problem for theory is the complexity of the energy surfaces for these clusters and the vast number of local minima they are likely to contain. Various search strategies, coupled with a number of theoretical approaches, have been used to explore clusters in this size range, resulting in a wide variety of cluster models.[6–12] As was true for the clusters with $N \leq 10$, definitive identification of the structures is likely to come only through a combination of theory and experiment.

In this paper we describe low-energy models for Si_{20} and Si_{21}, obtained using the local density approximation (LDA). These two structures have larger binding energies than alternative models that have appeared in the literature, making them leading candidates for minimum-energy structures. To further investigate the nature of these models and to encourage experimental work on clusters in this size range, we have computed the full vibrational spectrum for the clusters and the Raman and IR activities of the various modes. These calculations provide signatures that could be used to identify the clusters in experiments.

The structures we report here were obtained using a standard conjugate-gradient algorithm with atomic forces calculated within the LDA. Our computational approach has been presented elsewhere.[15] Gaussian orbitals are used to represent the electronic states of the clusters and a numerical scheme is used to obtain accurate LDA forces and total energies.[15] The cluster geometries were relaxed until the largest force on every atom dropped below 0.001 hartree/Bohr. Calculations performed here utilized a basis set of six *s*-type, five *p*-type, and three *d*-type orbitals on each Si atom [a ($6s5p3d$) basis]. The orbitals are contracted from a set of 15 even-tempered basis functions ($0.0654 \leq \alpha_i \leq 58800$). Based on calculations on smaller silicon clusters with this basis ($6s5p3d$) and a much larger basis ($9s8p6d$), we expect that the binding energies presented here are approximately 0.05 eV/atom above the exact LDA binding energies. The effect of the basis set on vibrational properties is discussed below.

For Si_{20}, we began with a starting structure that features three-fold coordinated atoms that had been obtained in an earlier symmetry-constrained search.[9] Removing the constraints, the structure relaxed to the geometry depicted in Fig. 1. Si_{20} can be viewed as roughly cylindrical in shape, with two seven-atom caps and a central six-atom ring. The cap atoms are close packed and highly coordinated, resembling small Si clusters. The central ring is more open and reminiscent of bulk Si. The average coordination of the atoms is 3.8 (where interatomic distances of less than 5.0 a.u. are identified as bonds), compared to 3.0 for the starting structure. An interesting feature is the negative curvature of the cluster surface connecting the caps to the central rings. This curvature directs nonbonded orbitals into the cluster interior where they could contribute to strengthening overall cluster binding. The electronic structure of this cluster is closed shell, with a highest occupied molecular orbital–lowest unoccupied molecular orbital (HOMO-LUMO) gap of 0.84 eV. With respect to spin-polarized isolated atoms, we calculate the cohesive energy of the Si_{20} cluster to be -4.37 eV/atom.

For Si_{21} we began the conjugate-gradient optimization from a structure that is analogous to the endohedral carbon fullerene clusters. It features a central atom surrounded by a highly symmetric cage of 20 atoms. The geometry was first
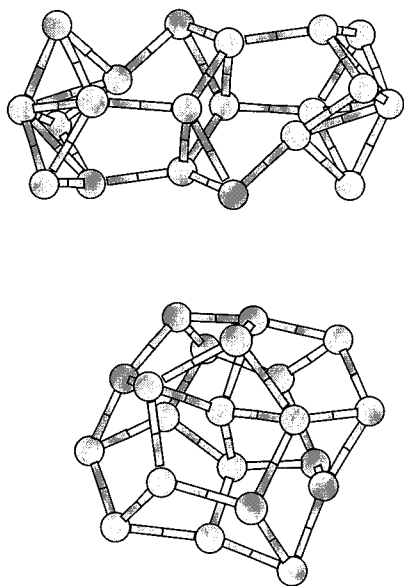
FIG. 1. Shown are the lowest-energy geometries for Si_{20} and Si_{21} that we have found.

relaxed maintaining the reflection symmetries of the cage. Once this structure was found, its dynamical matrix was computed and diagonalized, revealing three imaginary modes. The symmetry constraints were then removed, the cluster was displaced by a small distance along each imaginery mode, and the cluster was allowed to relax further, resulting in the structure shown in Fig. 1. In this structure the cage is significantly distorted, although the pentagonal rings associated with the original dodecahedral shell are still apparent in the figure. The relaxed structure retains one reflection plane and has an average coordination of 3.7. The electronic structure of this cluster is also closed shell, with a HOMO-LUMO gap of 0.54 eV. Using the same basis set as above we find the binding energy of Si_{21} to be -4.40 eV/ atom.

The large binding energy of this cluster is related to that of endohedral fullerene clusters[16] and very closely related to a novel $Zr@Si_{20}$ structure that was recently discovered.[17] The bonding in all these systems depends on a detailed match between the angular character of cage states near the Fermi level and the valence orbitals of the endohedral atom. These conditions are satisfied by an endohedral Si inside dodecahedral Si_{20};[17] however, in this case the Si atom is too small to completely fill the interior of the cage, and the cage distorts to the structure depicted in Fig. 1.

The results of our calculations indicate that the models shown in Fig. 1 are relatively stable. For example, while other LDA-based models for Si_{21} have not been published the structure shown in Fig. 1 is more stable than the published energetics for Si_{20}, Si_{22}, and the Si_{20} cluster discussed above. For example, in Ref. 6, a low-energy Si_{22} model is found to be less stable than Si_{20} by 0.07 eV/atom. Since our Si_{21} model is more stable than Si_{20} by 0.03 eV, we expect that it is a very good candidate for the lowest Si_{21} geometry. We have further tested the relative stability of this structure by considering a number of other models for Si_{21}. First, we have considered the possibility of placing a single silicon atom in the central void of the Si_{20} cluster

shown in Fig. 1. After relaxing this structure we converge to a geometry that is above our endohedral structure by 3.37 eV. We have also considered a structure that is akin to the elongated Grossman-Mitas Si_{20} geometry[7] with an additional atom placed in the central void. The relaxed version of this structure is also higher in energy, by 1.27 eV. We have also looked at seven-layer structures composed of stacked triangles (both staggered and eclipsed), and several different tetrahedral clusters that could be considered as a 17-atom silicon crystallite with four adatoms. All of these structures were well above the endohedral structure in energy. We now discuss energetic differences between Si_{20} isomers.

The structure presented in Fig. 1 (A) has one reflection plane plus inversion symmetry, which leads to a total of four symmetry operations. In Ref. 6, a low-energy structure (B) with the same symmetry but a different stacking sequence has been reported to be significantly more stable than the Si_{20} dodecahedron (3.6 eV) and more stable (1.9 eV) than a higher symmetry parent of structure (A).[9] It is not possible to continuously distort structure (A) into structure (B) without lowering the symmetry. To make a direct comparison of the energetic stability, we have recalculated the energy of structure (B) with our basis set and find it to be 0.36 eV higher than structure (A). We have also removed the inversion symmetry for structure (B) and allowed it to relax further, which leads to a structure that is only 0.2 eV above structure (A). Thus, the structure presented here is clearly a strong candidate for the minimum energy geometry for Si_{20}.

The near degeneracy of at least two Si_{20} isomers taxes the intrinsic accuracy to the approximations to density-functional (DF) theory and highlights the need for alternative approaches for quantitatively determining the ground-state structure of a cluster. The DF-based determination of vibrational spectra allows for such a means in many cases. Also, by determining the vibrational modes, the question of local stability of a cluster is addressed. Neither of these points has been discussed in previous density-functional-based calculations on clusters in this size regime so we now discuss these two points and apply this approach to our lowest-energy geometries for the lowest 20- and 21-atom clusters.

To compute the vibrational modes of these clusters, we diagonalized the full dynamical matrices, which are obtained by using Hellmann-Feynman-Pulay forces and the finite-differencing technique described in Ref. 18. Our previous LDA calculations on C_{60} have shown this technique to yield vibrational frequencies that are within about 10 cm^{-1} of the measured frequencies. Similar conclusions for LDA-based calculations on hydrocarbon molecules are presented in Ref. 19.

To obtain IR absorption and Raman activities for Si_{20} and Si_{21}, we use a new DF-based algorithm due to Porezag and Pederson, which has recently been shown to be accurate for applications on five small molecules.[20] A useful feature of this method is that, once the vibrational modes are determined, the Raman and IR intensities are obtained with a total of twelve additional self-consistent field (SCF) calculations *regardless of system size*. In this method, changes in dipole moments μ and the polarizability tensor (α_{xy}) as a function of normal-mode displacement (Q_i) are calculated directly and the IR intensities and Raman activities for the corresponding vibrational modes are extracted from the results.

TABLE I. Vibrational frequencies and Raman-IR intensities for the rhombohedral Si_4 cluster versus the basis set used. Units are cm^{-1} for frequencies (ω) and $Debye^2/amu/Å^2$ and ($Å^4/amu$) for IR and Raman line strengths (I), respectively. See text and Ref. 20 for more detail.

Activity	(9s8p6d)		(6s5p3d)		(5s4p)	
	ω	I	ω	I	ω	I
IR	53	0.12	40	0.11	100	0.06
IR	249	0.03	251	0.03	200	0.001
Raman	346	32.7	348	32.9	317	51.8
Raman	436	11.9	440	11.8	395	12.3
Raman	470	128.9	476	130.6	430	134.8
IR	496	1.34	502	1.36	463	1.57

TABLE II. Comparison of relative Raman cross sections as calculated within the LDA (our work), MP2, and from experiment. Cross sections depend on the Raman scattering activity, the vibrational and laser frequencies, and on temperature. Experimental results are from Fig. 2 of Ref. 5 and were obtained at $T=15$ K with a laser wavelength of 488 nm. Under these conditions, the Raman cross section will be mainly determined by the scattering activity and the vibrational frequency ω. Hence, the LDA S factor is found by multiplying the activities from Table I ($9s8p6d$) by $346/\omega \times I(\omega)/I(346)$. The MP2 results are from Table I of Ref 5.

LDA		MP2		Expt.	
ω	S	ω	S	ω	S
470	2.90	463	5.0	470	2.87
436	0.29	440	0.5	—	0
346	1.0	337	1.0	345	1

To determine the required derivatives ($d\mu_x/dQ_i$ and $d\alpha_{xy}/dQ_i$) we make use of the following:

$$\frac{\partial \mu_x}{\partial R_k^n} = -\frac{\partial^2 E}{\partial G_x \partial R_k^n} = \frac{\partial F_k^n}{\partial G_x}, \tag{1}$$

$$\frac{\partial \widetilde{\alpha}_{xy}}{\partial R_k^n} = -\frac{\partial^3 E}{\partial G_x \partial G_y \partial R_k^n} = \frac{\partial^2 F_k^n}{\partial G_x \partial G_y}. \tag{2}$$

In the above equation, F_k^n is the Hellmann-Feynman-Pulay force acting on the kth component of the nth atom (R_k^n), G_x is one component of the external electric field, and E is the total energy. Thus, from the above equations, the normal-mode displacement vectors, and the chain rule for differentiation, it is possible to determine the derivatives with respect to each and every normal mode displacement. The first and second derivatives of the Hellmann-Feynman-Pulay forces with respect to field strength are accurately obtained by performing 12 different SCF calculations, as a function of electric-field strength and direction and then using finite-differencing techniques to determine the derivatives. A complete account of this work appears in Ref. 20.

To demonstrate the accuracy of our first-principles calculation for the silicon-based systems studied here, we have calculated the Raman and IR spectra of the Si_4 cluster, which has been treated elsewhere in the literature.[5] Since the ground state of the Si_4 cluster is a planar rhombus, the vibrational modes are either Raman active or IR active but not both. The results of Table I show our LDA-based frequencies, infrared absorption intensities, and Raman scattering activities as calculated with three different basis sets. These results show that converged vibrational phenomena may be obtained using the ($6s5p3d$) basis set (36 functions per atom). We calculate the Raman-active modes to be at 470, 436, and 346 cm^{-1}. The high- and low-energy peaks agree very well with the experimental peaks at 470 and 345 cm^{-1}. In Table II, we compare our calculated results for the Raman cross sections with the Moller-Plesset perturbation theory (MP2) and experimental results which are both found in Ref. 5 The agreement between the three methodologies is quite good. In the experiments, the weak Raman mode at 436 cm^{-1} was not observed. The relative strengths of the two strong modes are 2.87:1, 5:1, and 2.9:1 within experiment,

MP2, and LDA, respectively. Based on the calculations in Ref. 20, the excellent agreement between LDA and experiment is better than expected. Regardless, it is clear that comparison of theoretical vibrational spectra and experimentally measured spectra will allow for experimental verification of theoretical structures. While we are not aware of any other researchers who have reported DF-based Raman activities and IR intensities for silicon clusters, we note that Chelikowsky, Glassford, and Phillips[10] have calculated the frequencies of the Raman-active modes of Si_4 to be 480, 460, and 340 cm^{-1} while Fournier, Sinnot, and DePristo found the same frequencies to be 464, 436, and 348 cm^{-1}, all in good agreement with the results reported here.[13,14]

Figure 2 displays the results obtained for the vibrational density of states (DOS) and the corresponding IR and Raman activities for Si_{20} and Si_{21}. For presentation purposes, we use a 10-cm^{-1} Gaussian broadening of the discrete cluster vibrational frequencies and weight the DOS according to

$$D(E) = \Sigma_i W(\omega_i) e^{-[(E-\omega_i/\gamma)]^2}, \tag{3}$$

where γ is the empirically chosen broadening factor (10 cm^{-1}), and W depends on whether the Raman, IR, or total DOS is being represented. Specifically, $W=1$ for the total density of states, $W=|d\vec{\mu}/dQ_i|^2$ for the infrared density of states, and $W=45(\partial\alpha/\partial Q)^2 + 7(\partial\beta/\partial Q)^2$ for Raman scattering. Here, Q is the normal-mode displacement, α and β are the isotropic and anisotropic parts of the polarizability tensor, and μ is the dipole moment of the cluster. For details see Ref. 20.

From Fig. 2 it can be seen that the DOS in both structures spans the range from 0 up to about 500 cm^{-1}. The DOS for Si_{20} has more structure, consistent with its more complex bonding structure. Both clusters have $3N-6$ real vibrational modes, indicating that they represent locally stable structures. The Si_{20} spectrum includes several low-frequency modes. The lowest, at about 20 cm^{-1}, is a bending mode that features the two caps translating together in one direction and the middle ring in the other, in a sausagelike fash-
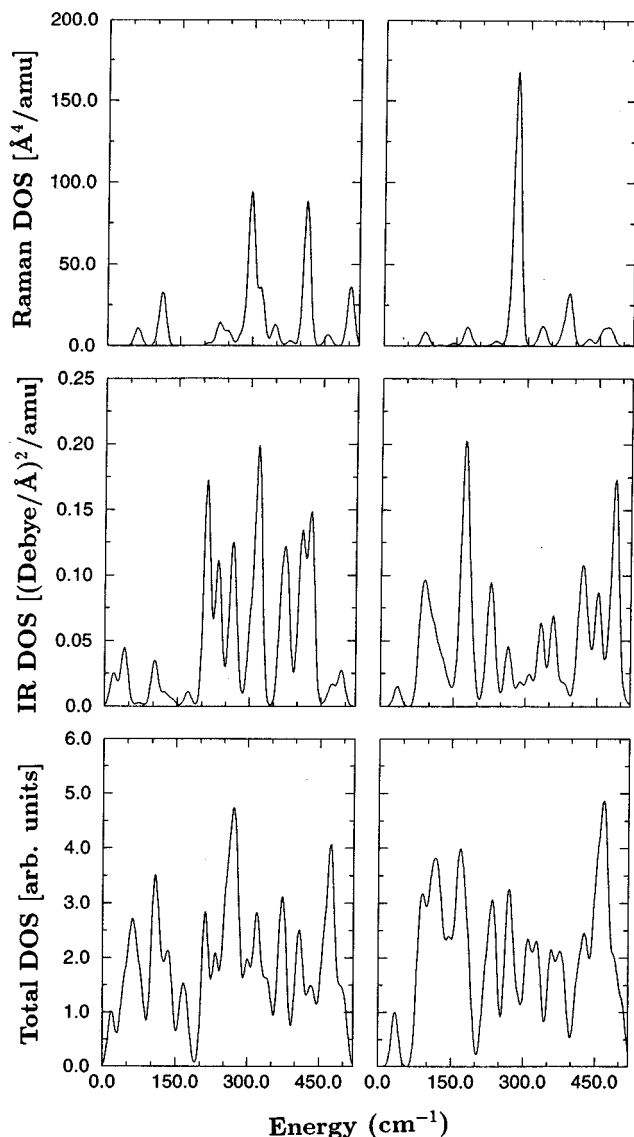
FIG. 2. Shown are the predicted vibrational spectra for our lowest-energy Si_{20} (left) and Si_{21} (right) geometries. The total, infrared, and Raman density of states are shown in the bottom, middle, and upper panels respectively.

ion. The effective mass of this mode is large, contributing to the low frequency. The other low frequencies are similar bending modes that have large effective masses.

In the IR, Si_{20} has six strong peaks at intermediate energies and weak peaks at low and high energies. In contrast, Si_{21} has strong IR activity at low and high energies and weak activity at intermediate energies. This qualitative difference should be easily resolved experimentally.

The most striking difference between the results for Si_{20} and Si_{21} are the Raman activities. Si_{20} has two dominant peaks at 295 and 412, and three somewhat less-pronounced peaks at 112, 320, and 505 cm^{-1}. The two strongest peaks correspond to breathing modes of the central ring and the two end caps, respectively. In contrast, Si_{21} has a single prominent peak at 275 cm^{-1}, corresponding to the breathing of the distorted cage about the central atom. The fact that there are only a small number of well-spaced Raman-active modes for each cluster implies that the theoretical predictions should be easily compared with experiment, and thus that the Raman spectra should be a useful probe of cluster structure.

Based on the results given above for Si_4, we expect that the calculated Raman and IR spectra for Si_{20} and Si_{21} should be in good agreement with experimental observations made for these clusters. The results shown in Fig. 2 thus represent predicted Raman and IR signatures for these cluster models that could be used to identify these clusters in experiments.

In summary, we have presented LDA-based results for low-energy Si_{20} and Si_{21} clusters. In addition to the fact that these clusters are the lowest-energy clusters obtained to date to our knowledge, these calculations represent the first DF-based models of intermediate-sized silicon clusters that are guaranteed to be at least locally stable (i.e., no imaginary vibrational modes). Further, the calculation of IR and Raman intensities within the DF method has not been applied to clusters in this size regime. The sharp contrast between the two vibrational spectra demonstrates that comparison of DF-based and experimental vibrational spectroscopy can provide an alternative approach to identifying ground-state geometries. Further, by concentrating on physical observables, this approach effectively bypasses questions about cluster stability and reactivity. Since DF-based calculations are generally more efficient than other formally exact quantum-mechanical approaches, such comparisons may provide the most cost effective means for determining ground-state geometries even in the few cases where the *approximations* to the exact DF theory lead to energetic results of insufficient accuracy.

[1] M. F. Jarrold, Science **252**, 1085 (1991), and references therein; K.-D. Rinnen and M. L. Mandich, Phys. Rev. Lett. **69**, 1823 (1992); J. E. Elkind *et al.*, J. Chem. Phys. **87**, 2397 (1987); M. F. Jarrold, Y. Imri, and U. Ray, *ibid*. **94**, 3607 (1991); J. M. Alford *et al.*, *ibid*. **94**, 2618 (1991).

[2] K. Raghavachari, Phase Transitions **24-26**, 61 (1990).

[3] N. Binggeli and J. R. Chelikowsky, Phys. Rev. B **50**, 11 764 (1994).

[4] U. Röthlisberg, W. Andreoni, and P. Giannozzi, J. Chem. Phys. **96**, 1248 (1991).

[5] E. C. Honea, A. Ogura, C. A. Murray, K. Raghavachari, W. O. Sprenger, M. F. Jarrold, and W. L. Brown, Nature **366**, 42 (1993).

[6] J. C. Grossman and L. Mitas, Phys. Rev. Lett. **74**, 1323 (1995).

[7] J. C. Grossman and L. Mitas, Phys. Rev. B **52**, 16 735 (1995).

[8] U. Rothlisberger, W. Andreoni, and M. Parrinello, Phys. Rev. B **72**, 665 (1992).

[9] E. Kaxiras and K. Jackson, Phys. Rev. Lett. **71**, 727 (1993).

[10] J. R. Chelikowsky, K. M. Glassford, and J. C. Phillips, Phys. Rev. B **44**, 1538 (1991).

[11] P. Ordejon, D. Lebedenko, and M. Menon, Phys. Rev. B **50**, 5645 (1994).

[12] T. T. Rantala, D. A. Jelski, and T. F. George, Chem. Phys. Lett. **232**, 215 (1995).

[13] X. Jing *et al.*, Solid State Commun. **96**, 231 (1995).

[14] R. Fournier, S. B. Sinnot, and A. E. DePristo, J. Chem. Phys. **97**, 4149 (1992).

[15] M. R. Pederson and K. A. Jackson, Phys. Rev. B **41**, 7453 (1990); K. A. Jackson and M. R. Pederson, *ibid.* **42**, 3276 (1990); M. R. Pederson and K. A. Jackson, *ibid.* **43**, 7312 (1991); in *Density Functional Methods in Chemistry*, edited by J. K. Labanowski and J. W. Andzelm (Springer-Verlag, Berlin, 1991);

[16] B.I. Dunlap, O. D. Haeberlen, and N. Roesch, J. Chem. Phys. **96**, 9095 (1992); M. R. Pederson and N. Laouini, Phys. Rev. B **48**, 2733 (1993); K. Jackson, E. Kaxiras, and M. R. Pederson, *ibid.* **48**, 17 556 (1993); J. Phys. Chem. **98**, 7805 (1994).

[17] K. A. Jackson and B. Nellermore (unpublished).

[18] M. R. Pederson, A. A. Quong, J. Q. Broughton, and J. L. Feldman, Comput. Mat. Sci. **2**, 536 (1994); A. A. Quong, M. R. Pederson, and J. L. Feldman, Solid State Commun. **87**, 535 (1993).

[19] M. R. Pederson, Chem. Phys. Lett. **230**, 54 (1994); D. Porezag and M. R. Pederson, J. Chem. Phys. **102**, 23 (1995).

[20] D. V. Porezag and M. R. Pederson, Phys. Rev. B (to be published).